Journal of Biomolecular NMR, 4 (1994) 845–858
ESCOM

J-Bio NMR 210

Backbone ^{1}H and ^{15}N resonance assignments of the N-terminal SH3 domain of drk in folded and unfolded states using enhanced-sensitivity pulsed field gradient NMR techniques

Ouwen Zhang[a,b], Lewis E. Kay[b], J. Paul Olivier[c] and Julie D. Forman-Kay[a,*]

[a]*Biochemistry Research Division, Hospital for Sick Children, 555 University Avenue, Toronto, ON, Canada M5G 1X8*
[b]*Protein Engineering Network Centres of Excellence and Departments of Medical Genetics, Biochemistry and Chemistry, University of Toronto, Toronto, ON, Canada M5S 1A8*
[c]*Division of Molecular and Developmental Biology, Samuel Lunenfeld Research Institute, Mount Sinai Hospital, 600 University Avenue, Toronto, ON, Canada M5G 1X5*

Received 24 May 1994
Accepted 13 June 1994

Keywords: ^{15}N chemical shifts; Unfolded state; Pulsed field gradients; Sensitivity enhanced; Water suppression; SH3 domain

SUMMARY

The backbone ^{1}H and ^{15}N resonances of the N-terminal SH3 domain of the *Drosophila* signaling adapter protein, drk, have been assigned. This domain is in slow exchange on the NMR timescale between folded and predominantly unfolded states. Data were collected on both states simultaneously, on samples of the SH3 in near physiological buffer exhibiting an approximately 1:1 ratio of the two states. NMR methods which exploit the chemical shift dispersion of the ^{15}N resonances of unfolded states and pulsed field gradient water suppression approaches for avoiding saturation and dephasing of amide protons which rapidly exchange with solvent were utilized for the assignment.

INTRODUCTION

NMR has been shown to be very useful for studying the structure of unfolded states of proteins and partially folded equilibrium 'intermediates', as well as folded forms. NMR analyses of rates of amide hydrogen exchange, NOE data and chemical shifts of denatured and intermediate states

*To whom correspondence should be addressed.

Abbreviations: 2D, 3D, two-, three-dimensional; drkN SH3, N-terminal SH3 domain of *Drosophila* drk; HSQC, heteronuclear single-quantum spectroscopy; NOE, nuclear Overhauser enhancement; SH3, Src homology domain 3; TOCSY, total correlation spectroscopy.

have been successful in identifying regions of native-like structure for certain proteins (Evans et al., 1991; Neri et al., 1992). The structure and dynamics of a denatured 131-residue fragment of staphylococcal nuclease was characterized using NOEs, coupling constants and amide temperature coefficients, showing regions of persistent native-like secondary structure (Alexandrescu et al., 1994). In a study by Lumb and Kim (1994), denatured bovine pancreatic trypsin inhibitor was found to maintain a native-like hydrophobic cluster. A difficulty in studying unfolded proteins by NMR has been the poor ^{1}H chemical shift dispersion. This has been compounded by the need to find conditions of slow chemical exchange with the native state, in order to transfer native assignments to the unfolded form. Recently, triple-resonance 3D NMR methods have been applied to direct chemical shift assignment and characterization of unfolded states, avoiding the necessity of transferring assignments from the native state (Logan et al., 1993,1994). This is possible since the dispersion of ^{15}N chemical shifts, in particular, is less affected by unfolding than that of proton shifts, the increase in dimensionality allows for greater resolution of the resonances and the use of triple-resonance methods enables the assignment to be independent of structure-based NOEs, which can be weak in unfolded states.

Nevertheless, the study of folding intermediates and unfolded states of proteins by NMR poses significant challenges. Folding intermediates often exhibit very broad lines, due to intermediate rates of exchange between a number of accessible conformational states. Since both folding intermediates and unfolded states of proteins display much more rapid NH exchange with water than stably folded states, NMR methods for their study must utilize solvent suppression techniques which do not significantly saturate the amide resonances. The recent development of pulsed field gradient techniques for high-resolution protein applications enables their use for these conformationally labile systems. In addition, the extremely poor proton chemical shift dispersion of resonances of the unfolded state requires the use of isotopic labeling and heteronuclear NMR approaches, even for relatively small protein systems.

We have applied heteronuclear NMR techniques to the study of folded and unfolded states of the isolated N-terminal Src homology 3 (SH3) domain of drk, the *Drosophila* signal transduction protein. This modular protein of 23 kDa is composed of a central Src homology 2 (SH2) domain, surrounded by two SH3 domains (Olivier et al., 1993; Simon et al., 1993). SH3 sequences are found in proteins involved in signal transduction and cytoskeletal localization (Koch et al., 1991). These domains, of 50–70 residues in length, mediate interactions in signaling (Cicchetti et al., 1992; Musacchio et al., 1992a; Pawson and Gish, 1992) by binding to left-handed type II polyproline helix regions of target proteins (Yu et al., 1994). A number of isolated SH3 domains have been expressed in bacteria and have been observed to fold independently into a functional form. Structures have been determined for isolated SH3 domains of chicken brain spectrin (Musacchio et al., 1992b), src (Yu et al., 1992), phospholipase C-γ1 (Khoda et al., 1993), the p85 subunit of phosphoinositol-3'-kinase (Booker et al., 1992; Koyama et al., 1993), fyn (Noble et al., 1993) and GTPase-activating protein (Yang et al., 1994). In addition, the structure of the p85 SH3 complexed with a proline-rich peptide has also been determined (Yu et al., 1994). These structures are highly homologous, with a topology of a β-sandwich of two orthogonal β-sheets.

In this paper, we present the backbone proton and ^{15}N resonance assignments of the isolated N-terminal SH3 of drk in folded and unfolded states, as well as new approaches and pulsed field gradient NMR experiments useful for the assignment of folded and unfolded states of proteins. These techniques allow excellent solvent suppression, while minimizing saturation and dephasing

of the water resonance. In this way amide proton saturation via exchange with water, which is particularly detrimental to the study of the labile unfolded state, is avoided. We describe enhanced-sensitivity pulsed field gradient versions of the ^{15}N-edited TOCSY-HSQC and NOESY-HSQC experiments, as well as a new 3D ^{15}N HSQC-TOCSY-NOESY-HSQC experiment. All experiments minimize saturation of water through the combined use of water-selective pulses and gradients, as has been described previously (Grzesiek and Bax, 1993; Kay et al., 1994). The latter pulse sequence takes full advantage of the chemical shift dispersion of amide ^{15}N resonances in unfolded states to resolve overlapping peaks in a sample containing an equilibrium between folded and unfolded states, and has proven to be useful for sequential assignment. The data obtained from these ^{15}N-edited experiments have been utilized for the determination of the secondary structure and overall topology of the SH3 in the folded state and a characterization of its structure in a predominantly unfolded state, populated under physiological conditions (Zhang and Forman-Kay, 1994).

MATERIALS AND METHODS

Expression, purification and sample preparation

The gene fragment coding for residues 1 through 59 of the original drk clone (Olivier et al., 1993), comprising the N-terminal SH3 of drk (drkN SH3), was subcloned, expressed and purified as described elsewhere (Zhang and Forman-Kay, 1994). NMR samples contained 0.5–1.0 mM drkN SH3 in 50 mM sodium phosphate, pH 6.0, 90% H_2O/10% D_2O. Addition of 50 mM Na_2SO_4 to some samples was used to help prevent aggregation of the SH3 domain over long periods of time at room temperature or above.

NMR spectroscopy

Experiments were performed on Varian Unity 500 MHz spectrometers, equipped with actively shielded Z-gradient probes and gradient amplifier units. Data were processed and analyzed on SUN SparcStations using Varian VNMR software, nmrPipe/nmrDraw software, recently developed by F. Delaglio at the NIH (Delaglio, 1993) and PIPP (Garrett et al., 1991).

Figure 1 illustrates the pulse schemes that were used in the present study. Pulsed field gradients were used to minimize the artifact content of the spectra (Bax and Pochapsky, 1992) and to select for the coherence transfer pathway traversing nitrogen, using an enhanced-sensitivity (Palmer et al., 1991) gradient approach described previously (Kay et al., 1992; Schleucher et al., 1993; Muhandiram and Kay, 1994). In addition, saturation of water was minimized through the use of 'water-selective pulses' and gradients and by ensuring that water magnetization is placed along the +z-axis immediately prior to acquisition (Grzesiek and Bax, 1993; Kay et al., 1994). The acquisition time, t_2 for the 2D HSQC or t_3 for all 3D experiments, was 64 ms with 1K data points and a relaxation delay of 1.0 s. For the HSQC spectra, 128 complex t_1 increments were recorded. Spectral widths were 1650 Hz in F_1 and 8000 Hz in F_2. For the TOCSY- and NOESY-HSQC experiments, 128 complex t_1 and 64 complex t_2 increments were recorded using 8 scans, with spectral widths of 5500 Hz (F_1), 1500 Hz (F_2) and 8000 Hz (F_3). The TOCSY utilized a mixing time of 55 ms for a total measuring time of ~ 75 h and in the NOESY, a mixing time of 150 ms was used with a total measuring time of ~ 95 h. The HSQC-TOCSY-NOESY-HSQC was recorded with 64 complex t_1 and 48 complex t_2 increments, using 16 scans and spectral widths of 1500 Hz (both

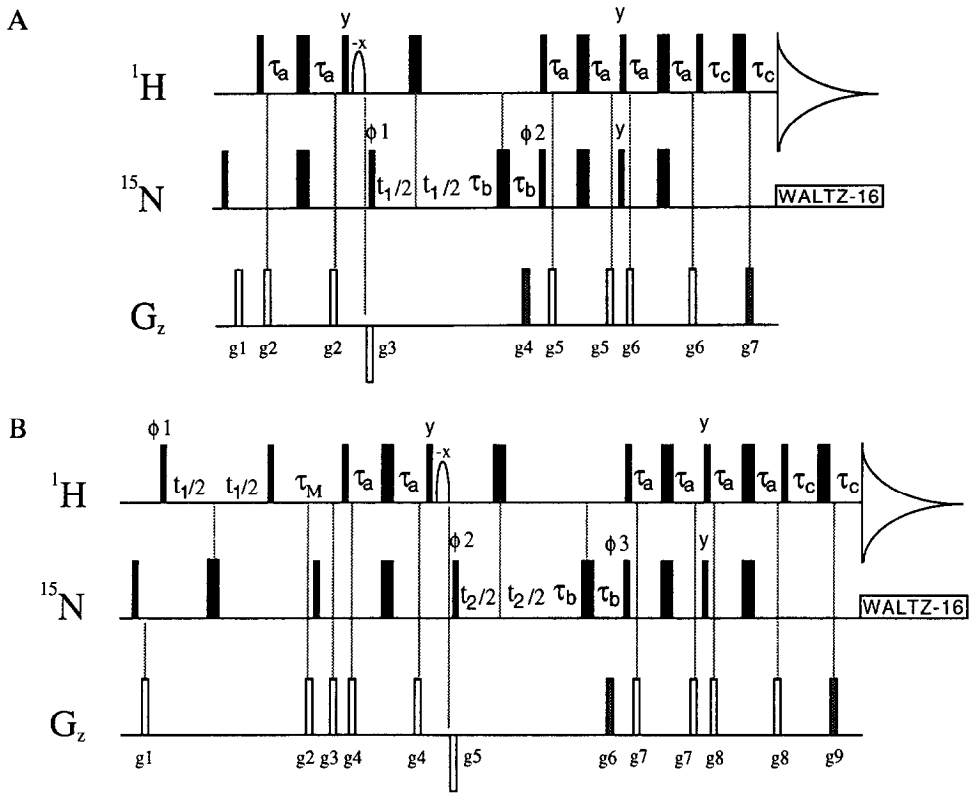

Fig. 1. Pulse schemes for (A) gradient-enhanced ^{15}N HSQC; (B) gradient-enhanced ^{15}N NOESY-HSQC; (C) gradient-enhanced ^{15}N TOCSY-HSQC; and (D) gradient-enhanced ^{15}N HSQC-TOCSY-NOESY-HSQC. Narrow pulses represent a flip angle of 90°, while wide pulses correspond to a flip angle of 180°. Pulses for which the phases are not indicated are applied along the x-axis. In all pulse schemes, water saturation/dephasing is minimized through the use of 'water-selective' pulses (shaped pulses in the figure) (Grzesiek and Bax, 1993; Kay et al., 1994) which are 2 ms in duration and have either a rectangular profile or the profile of a SEDUCE-1 90° element (McCoy and Mueller, 1992). The ^{1}H carrier is placed on the water resonance for the duration of the experiment. Nonselective ^{1}H pulses are applied with a 23.5 kHz field, while a field of 9.5 kHz is employed for the DIPSI-2rc (Cavanagh and Rance, 1992) mixing scheme (note that the 14th pulse in this reference should be 255° and not 225°). The ^{15}N pulses are applied with a field of 5.5 kHz, with nitrogen decoupling during acquisition achieved through the use of a 1 kHz WALTZ decoupling field (Shaka et al., 1983). The delays τ_a, τ_b and τ_c were set to 2.3, 1.5 and 0.5 ms, respectively. For all sequences, two data sets are recorded (in an interleaved manner) with the phase of the gradient applied during the final τ_c period in each of the sequences inverted for each data set. The phase of the ^{15}N 90° pulse immediately following the first coherence transfer selection gradient (g4, g6, g4 and g9 in experiments A, B, C and D, respectively) is incremented by 180° when the phase of the gradient pulse is inverted (Kay et al., 1992). Postacquisition processing involving addition and subtraction of the N- and P-type data followed by a 90° zero-order phase correction of one (not both) of the data sets is accomplished using home-written software (Kay et al., 1992). The data sets are subsequently processed according to States et al. (1982) to yield pure absorptive spectra. The gradient pulses which are hatched are used to select for the appropriate transfer pathway. In scheme (A) the phase cycle is $\phi1 = (x,-x)$; $\phi2 = x$; rec = (x,−x). The gradient strengths and durations are: g1 = (1 ms, 4 G/cm), g2 = (750 μs, 5 G/cm), g3 = (1.5 ms, −15 G/cm), g4 = (1.25 ms, 30 G/cm), g5 = g6 = (500 μs, 4 G/cm), g7 = (125 μs, 27.8 G/cm). The phase of $\phi1$ is incremented by 180° along with the phase of the receiver for each increment of t_1. In scheme (B) the phase cycle is $\phi1 = (135°, 315°)$; $\phi2 = 2(x),2(-x)$; $\phi3 = x$; rec = x,2(−x),x. Quadrature in F_1 is obtained by the method of States et al. (1982). The values of $\phi1$ employed ensure that a significant component of the water magnetization is present in the transverse plane at the start of the mixing period, so that radiation damping can occur efficiently. In this way the water magnetization is restored to the +z-axis prior to the application of the gradient pulse g2. In this context, g2 is applied within the last 10 ms of the mixing

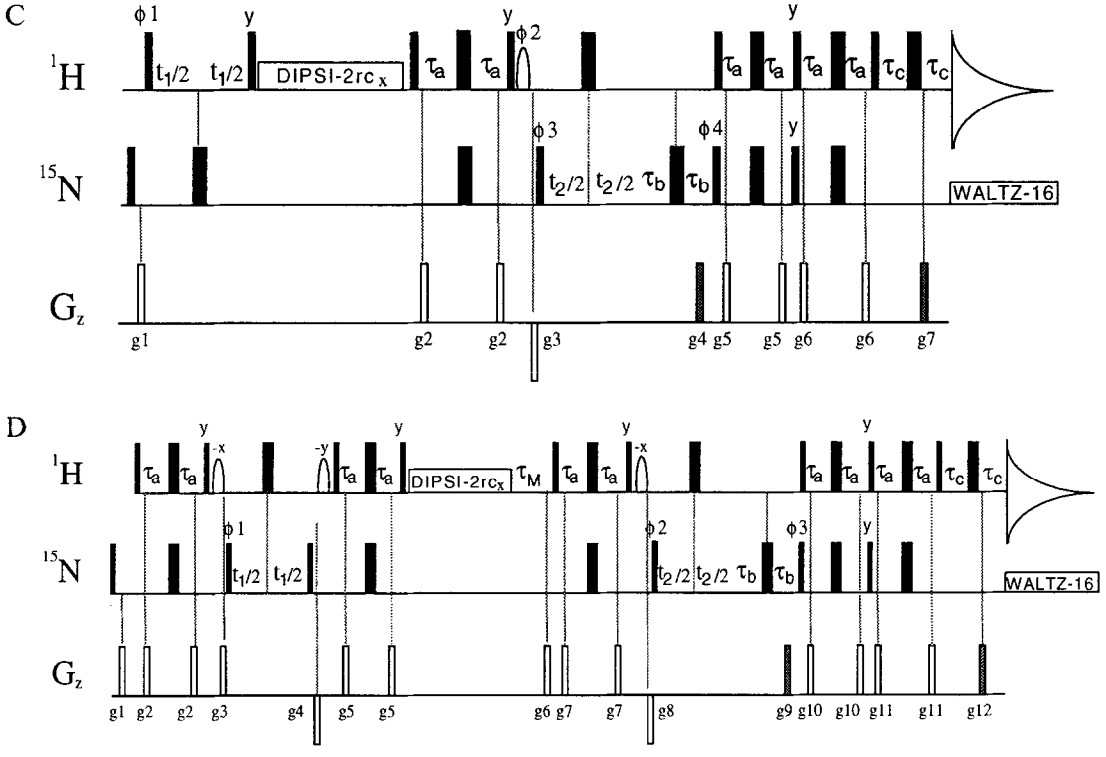

time. The phase of $\phi 2$ is incremented by 180° along with the phase of the receiver for each increment of t_2. The gradient strengths and durations are: g1 = (1 ms, 4 G/cm), g2 = (1 ms, 10 G/cm), g3 = (0.5 ms, 8 G/cm), g4 = (750 μs, 5 G/cm), g5 = (1.5 ms, −15 G/cm), g6 = (1.25 ms, 30 G/cm), g7 = g8 = (0.5 ms, 4 G/cm), g9 = (125 μs, 27.8 G/cm). In scheme (C) the phase cycle is $\phi 1 = (y,-y)$; $\phi 2 = (x,-x)$; $\phi 3 = 2(x),2(-x)$; $\phi 4 = x$; rec = x,2(−x),x. Note that when the phase of $\phi 1$ is incremented by 90° to obtain quadrature in F_1 by the method of States et al. (1982), the phase of $\phi 2$ is incremented by 270° (i.e., $\phi 2 = (-y,y)$ when $\phi 1$ is cycled (−x,x)). This ensures that dephasing of the water magnetization via the action of the gradients is minimized and that water is restored to the +z-axis immediately prior to detection. The phase of $\phi 3$ is incremented by 180° along with the phase of the receiver for each increment of t_2. The gradient strengths and durations are: g1 = (1 ms, 4 G/cm), g2 = (0.5 ms, 8 G/cm), g3 = (1.5 ms, −15 G/cm), g4 = (1.25 ms, 30 G/cm), g5 = g6 = (0.5 ms, 4 G/cm), g7 = (125 μs, 27.8 G/cm). In scheme (D) the phase cycle is $\phi 1 = (x,-x)$; $\phi 2 = 2(x),2(-x)$; $\phi 3 = x$; rec = x,2(−x),x. Quadrature in F_1 is obtained by States-TPPI (Marion et al., 1989). The gradient strengths and durations are: g1 = (1 ms, 4 G/cm), g2 = (0.5 ms, 2 G/cm), g3 = (1 ms, 15 G/cm), g4 = (0.5 ms, −7 G/cm), g5 = (0.5 ms, 5 G/cm), g6 = (1 ms, 8 G/cm), g7 = (500 μs, 2 G/cm), g8 = (1 ms, −10 G/cm), g9 = (1.25 ms, 30 G/cm), g10 = g11 = (0.5 ms, 4 G/cm), g12 = (125 μs, 27.8 G/cm). A delay of at least 50 μs is inserted between the application of a gradient pulse and the subsequent application of rf pulses.

F_1 and F_2) and 8000 Hz (F_3). The TOCSY mixing time was 30 ms and the NOESY mixing time 100 ms, giving a total measuring time of ~ 65 h.

RESULTS AND DISCUSSION

Equilibrium between folded and unfolded states of the SH3

The isolated N-terminal SH3 of drk was not stably folded, unlike other isolated SH3 domains and numerous other isolated domains of modular proteins. A 2D homonuclear TOCSY of 1 mM

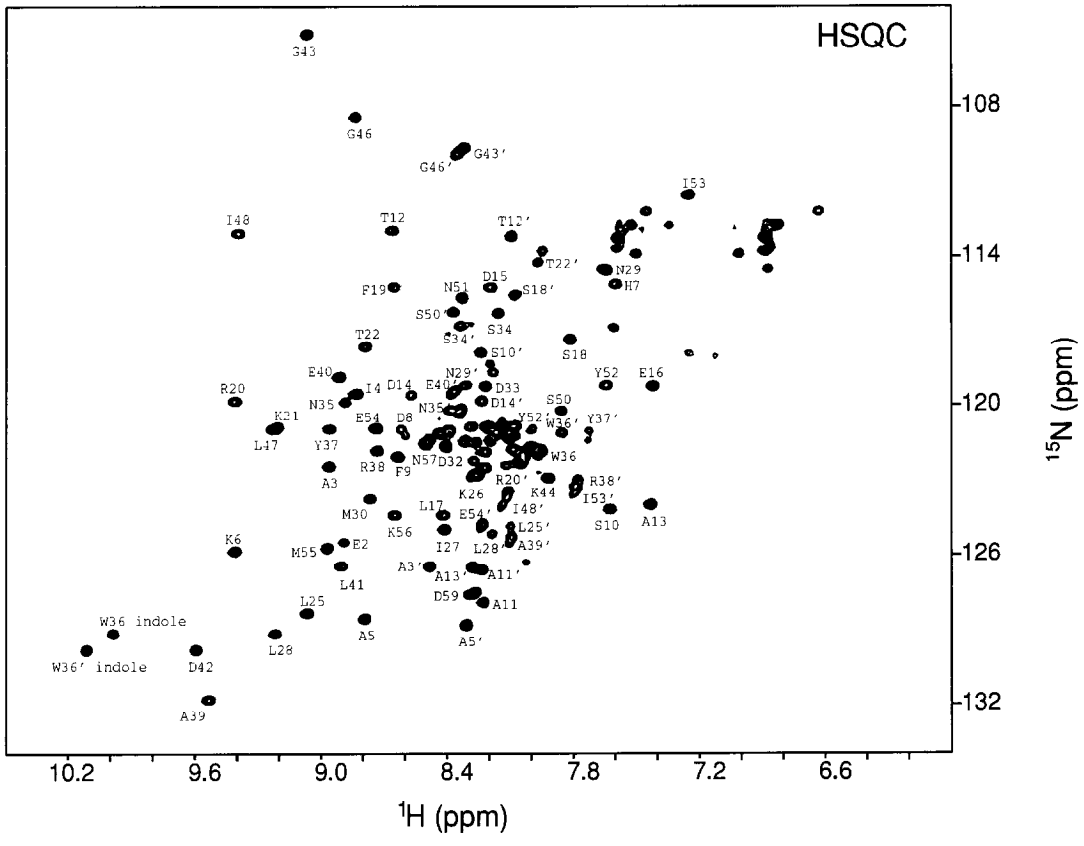

Fig. 2. ^{15}N-^{1}H HSQC spectrum of 1 mM drkN SH3 in 50 mM sodium phosphate, pH 6.0, 30 °C. Most backbone amide cross peaks have been labeled with the amino acid name (one-letter code); resonances of the unfolded form are also marked with a prime (′). Resonances of the side-chain glutamine and asparagine amide groups have not been labeled.

drkN SH3 in 50 mM sodium phosphate, pH 6.0, 30 °C (data not shown), contained a large number of amide–amide cross peaks. Upon examination of the spectrum, the presence of conformational exchange between folded and unfolded forms of the drkN SH3 became apparent, with a clustering of chemical shifts in one dimension between 8 and 8.5 ppm correlated with resonances ranging from 6.5 to 9.5 ppm in the other. In addition, the TOCSY showed two downfield resonances exhibiting a mutual exchange peak, which could be assigned to the side-chain indole proton of the single Trp^{36} residue of the SH3 in two distinct conformations. Twice the number of expected peaks for a folded protein of 59 residues was observed in ^{15}N-^{1}H HSQC spectra of the sample (Fig. 2). Conformational exchange between folded and unfolded states of the drkN SH3 domain was demonstrated by 1D and 2D HSQC titrations using conditions known to either destabilize or stabilize the folded structure of proteins, as described elsewhere (Zhang and Forman-Kay, 1994).

Resonance assignments and structural analysis of folded and unfoled states

Although the isolated SH3 domain comprises only 59 residues, isotopic labeling with ^{15}N was

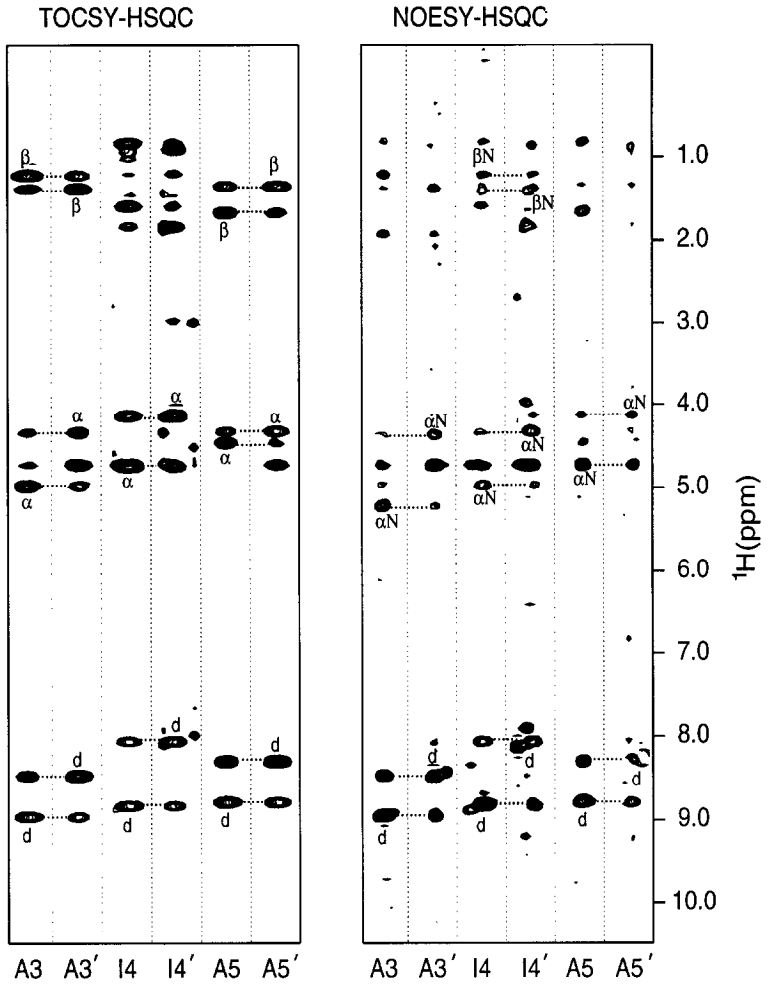

Fig. 3. Amide strips from the 3D ^{15}N TOCSY-HSQC and NOESY-HSQC experiments for resonances of Ala^3 to Ala^5 of folded and unfolded (') states of the drkN SH3 domain in 50 mM sodium phosphate, pH 6.0, 30 °C. Intraresidue $C^{\alpha}H_i$,NH_i and $C^{\beta}H_i$,NH_i TOCSY peaks are labeled α and β, respectively, while sequential $C^{\alpha}H_i$,NH_{i+1} and $C^{\beta}H_i$,NH_{i+1} NOESY peaks are labeled αN and βN, respectively. Diagonal peaks are labeled d and dotted lines connect the direct peaks with exchange peaks, including diagonal, TOCSY and NOESY exchange peaks.

necessary in order to resolve the clustered amide protons of the unfolded state resonating between 8 and 8.5 ppm. Sequential assignments of the resonances were made for both folded and unfolded states of the drkN SH3, using 3D ^{15}N NOESY-HSQC and TOCSY-HSQC experiments recorded on both forms simultaneously. The sample conditions were 1 mM protein in 50 mM sodium phosphate, pH 6.0 and 30 °C, giving an approximate 1:1 ratio between the two states. The chemical shift dispersion for ^{15}N in the unfolded state, which is almost unchanged from that in the folded state, allowed nearly complete resolution of peaks in the HSQC spectrum (see Fig. 2).

Approximately 80% of the backbone resonances of both the folded and unfolded forms were

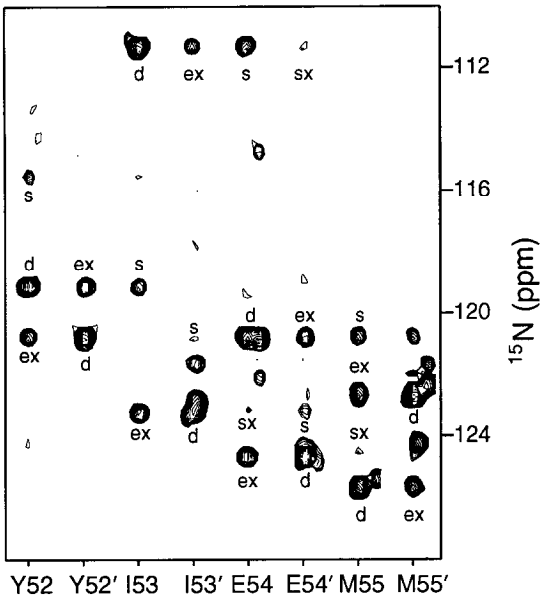

Fig. 4. Amide strips from the 3D ^{15}N HSQC-TOCSY-NOESY-HSQC experiment for residues Tyr^{52} to Met^{55} of folded and unfolded (') states of the drkN SH3 domain in 50 mM sodium phosphate, 50 mM Na_2SO_4, pH 6, 25 °C. Diagonal peaks (^{15}N(**f**)$_i$,NH(**f**)$_i$ or ^{15}N(**u**)$_i$,NH(**u**)$_i$ are marked 'd', exchange peaks (^{15}N(**f**)$_i$,NH(**u**)$_i$ or ^{15}N(**u**)$_i$,NH(**f**)$_i$) are marked 'ex', sequential TOCSY-NOESY peaks (^{15}N(**f**)$_i$,NH(**f**)$_{i+1}$ or ^{15}N(**u**)$_i$,NH(**u**)$_{i+1}$) are marked 's' and exchange sequential TOCSY-NOESY peaks (^{15}N(**f**)$_i$,NH(**u**)$_{i+1}$ or ^{15}N(**u**)$_i$,NH(**f**)$_{i+1}$) are marked 'sx'.

sequentially assigned using these 3D ^{15}N TOCSY-HSQC and NOESY-HSQC experiments. The assignment was aided by the presence of slow exchange between the folded and unfolded states of the protein. This enabled assignment of pairs of resonances from the two conformations to be made in tandem and gave rise to a potential for observing four TOCSY or NOESY cross peaks between any two protons a and b: (i) the direct ^{1}H(**f**)$_a$,^{1}H(**f**)$_b$ TOCSY/NOESY peak in the folded state; (ii) the direct ^{1}H(**u**)$_a$, ^{1}H(**u**)$_b$ TOCSY/NOESY peak in the unfolded state; (iii) a TOCSY or NOESY exchange peak between ^{1}H(**f**)$_a$ in the folded state and ^{1}H(**u**)$_b$ in the unfolded state; and (iv) a TOCSY or NOESY exchange peak between ^{1}H(**u**)$_a$ in the unfolded state and ^{1}H(**f**)$_b$ in the folded state. The additional complication in the spectrum from potentially four times the number of cross peaks was compensated for by the confirmation of spin system assignments from the exchange TOCSY peaks and of sequential assignments made possible by the observation of up to four times the number of sequential NOEs. Assignment of resonances to the folded or unfolded state was made based on a number of considerations, including the difference between the observed chemical shift and literature values for random coil chemical shifts, the intensity of the amide–water exchange peaks observed in the 3D NOESY-HSQC and TOCSY-HSQC experiments (Zhang and Forman-Kay, 1994), and the relative intensity of sequential NOE connectivities compared to previously assigned resonances. Figure 3 illustrates amide strips from these experiments for resonances of Ala^3, Ile^4 and Ala^5 of folded and unfolded states. Note the presence of four sequential $C^{\alpha}H_i$,NH_{i+1} and $C^{\beta}H_i$,NH_{i+1} cross peaks for some of these residues in the NOESY and the difference in the intensity of the amide–water exchange peaks for resonances of

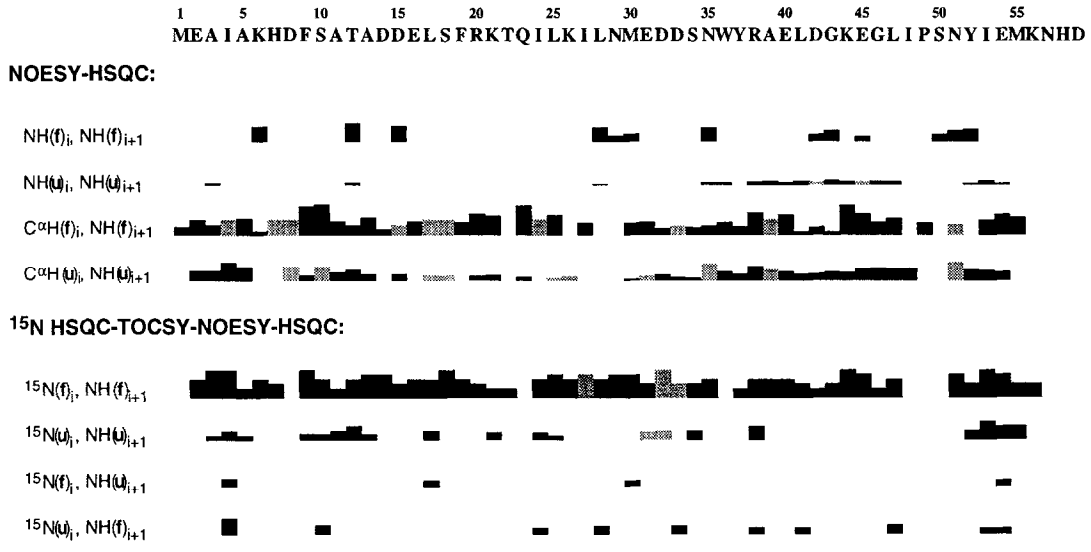

Fig. 5. Summary of the major sequential information derived from 3D ^{15}N NOESY-HSQC and ^{15}N HSQC-TOCSY-NOESY-HSQC experiments performed on the drkN SH3 domain.

folded and unfolded forms. While exchange TOCSY peaks (i.e., $^1H(\mathbf{f})_a$,$^1H(\mathbf{u})_b$, where ^1H_a and ^1H_b are part of the same spin system) were observed for almost all of the residues, exchange NOEs (i.e., $^1H(\mathbf{f})_a$,$^1H(\mathbf{u})_b$, where ^1H_a and ^1H_b are within 5 Å of each other) were only seen for about 10% of the residues. Direct exchange peaks (i.e., $^1H(\mathbf{f})_a$,$^1H(\mathbf{u})_a$) were also observed for almost every residue, with the exception of Glu^2, His^7, Asp^8 and the three C-terminal residues, for many of which no peaks of the unfolded state could be assigned.

In order to confirm and complete the assignments derived from the 3D ^{15}N NOESY-HSQC and TOCSY-HSQC data, an experiment which more fully exploited the ^{15}N chemical shift dispersion to resolve the overlapping peaks from the two states of the SH3 was designed, the ^{15}N HSQC-TOCSY-NOESY-HSQC. This experiment is based on the ^{15}N-edited 3D TOCSY-NOESY previously described by Mueller and co-workers (1992), but differs in that ^{15}N chemical shifts are recorded in two of the three dimensions. The TOCSY-NOESY experiment begins with magnetization on the amide proton of residue i, transfers this via the intraresidue HNC$^\alpha$H coupling to the C$^\alpha$H of the same residue in the TOCSY step and subsequently to the amide proton of residue i + 1 in the NOESY step. The experiment functions optimally for proteins having a predominantly extended β-structure, as in the folded state of SH3 domains. In this case, the large intraresidue HNC$^\alpha$H coupling of $\gtrsim$ 8 Hz leads to efficient TOCSY transfer from NH to C$^\alpha$H and the short distance of less than 2.5 Å between $C^\alpha H_i$ and NH_{i+1} facilitates the NOESY transfer step. For unfolded proteins, the $^3J_{HN^\alpha}$ value is between 6 and 7 Hz and NOEs between $C^\alpha H_i$ and NH_{i+1} are often observed, leading us to expect sequential cross peaks in the HSQC-TOCSY-NOESY-HSQC for some of the resonances of the unfolded state. In the HSQC-TOCSY-NOESY-HSQC experiment, the ^{15}N chemical shift of the nitrogen, which is one-bond correlated to the amide proton where magnetization originates, is recorded together with the ^{1}H and ^{15}N chemical shifts of the destination amide.

The ^{15}N HSQC-TOCSY-NOESY-HSQC experiment was recorded on a 1 mM sample of the

TABLE 1
BACKBONE CHEMICAL SHIFTS (ppm) OF FOLDED AND UNFOLDED STATES OF THE drkN SH3 DOMAIN[a]

Residue	Folded			Unfolded		
	NH	^{15}N	H^{α}	NH	^{15}N	H^{α}
Met[1]	[b]	[b]	4.18	[b]	[b]	[b]
Glu[2]	8.88	125.6	5.23	[b]	[b]	4.39
Ala[3]	8.96	122.6	4.98	8.48	126.3	4.34
Ile[4]	8.83	119.6	4.74	8.07	120.6	4.14
Ala[5]	8.78	128.7	4.47	8.30	128.6	4.33
Lys[6]	9.40	126.0	4.30	8.18	121.3	4.26
His[7]	7.59	115.2	4.67	8.42	121.3	4.26
Asp[8]	8.60	120.9	4.71	8.26	121.7	4.61
Phe[9]	8.62	122.1	4.69	8.25	121.6	4.63
Ser[10]	7.62	124.2	4.42	8.25	117.9	4.40
Ala[11]	8.23	128.0	3.87	8.22	126.6	4.40
Thr[12]	8.67	113.4	4.39	8.08	113.2	4.38
Ala[13]	7.46	124.2	4.59	8.27	126.6	4.34
Asp[14]	8.56	119.7	4.41	8.23	119.9	4.57
Asp[15]	8.21	115.3	4.73	8.21	121.0	4.58
Glu[16]	7.42	119.4	5.15	8.32	121.6	4.19
Leu[17]	8.45	124.7	4.72	8.11	121.4	4.25
Ser[18]	7.82	117.6	4.77	8.08	115.7	4.28
Phe[19]	8.65	115.3	4.97	8.04	122.1	4.54
Arg[20]	9.40	119.9	5.09	8.08	121.5	4.16
Lys[21]	9.20	121.0	3.55	8.11	121.0	4.21
Thr[22]	8.79	117.7	4.52	7.96	114.3	4.21
Gln[23]	8.12	121.3	4.32	8.12	121.3	4.27
Ile[24]	8.16	121.1	4.80	8.01	121.7	4.05
Leu[25]	9.06	128.4	4.65	8.09	124.7	4.27
Lys[26]	8.22	122.6	4.68	8.02	121.8	4.27
Ile[27]	8.42	125.1	4.18	7.95	122.0	4.09
Leu[28]	9.21	129.2	4.43	8.17	125.0	4.32
Asn[29]	7.64	114.6	4.80	8.31	119.2	4.71
Met[30]	8.76	123.8	4.43	8.27	120.9	4.45
Glu[31]	8.09	121.9	4.38	8.38	121.1	4.26
Asp[32]	8.41	121.8	4.47	8.14	121.0	4.58
Asp[33]	8.22	119.3	4.68	8.22	121.9	4.54
Ser[34]	8.15	116.4	4.53	8.33	116.6	4.33
Asn[35]	8.88	120.0	4.59	8.35	120.3	4.72
Trp[36]	8.00	121.8	5.20	7.86	121.1	4.56
Tyr[37]	8.96	121.1	5.37	7.72	121.0	4.35
Arg[38]	8.72	121.9	4.93	7.78	123.0	4.18
Ala[39]	9.54	131.9	5.47	8.09	125.4	4.21
Glu[40]	8.92	119.0	5.46	8.37	119.5	4.25
Leu[41]	8.90	126.5	4.71	8.04	122.4	4.33
Asp[42]	9.59	129.9	4.39	8.21	120.7	4.59
Gly[43]	9.08	105.2	3.68/4.23	8.31	109.7	3.98
Lys[44]	7.92	123.0	4.68	8.10	121.0	4.34
Glu[45]	8.42	121.1	5.78	8.48	121.4	4.28

TABLE 1 (continued)

Residue	Folded			Unfolded		
	NH	^{15}N	H^{α}	NH	^{15}N	H^{α}
Gly^{46}	8.84	108.6	3.95/4.16	8.34	109.9	3.95
Leu^{47}	9.23	121.1	5.44	7.95	121.8	4.38
Ile^{48}	9.39	113.2	5.14	8.10	123.4	4.47
Pro^{49}	–	–	5.18	–	–	–
Ser^{50}	7.87	120.3	4.55	8.34	116.5	4.35
Asn^{51}	8.33	115.7	4.74	8.33	120.3	4.74
Tyr^{52}	7.65	119.3	4.65	8.00	121.0	4.51
Ile^{53}	7.25	111.3	5.24	7.80	123.2	4.04
Glu^{54}	8.75	121.1	4.71	8.23	124.8	4.21
Met^{55}	8.97	125.8	4.56	8.26	122.7	4.47
Lys^{56}	8.64	124.5	4.38	8.24	122.8	4.33
Asn^{57}	8.48	121.5	4.73	[b]	[b]	[b]
His^{58}	8.18	118.8	4.73	[b]	[b]	[b]
Asp^{59}	8.26	127.7	4.44	[b]	[b]	[b]

[a] Assignments made in 50 mM sodium phosphate, pH 6, 30 °C, with water at 4.73 ppm as internal reference.

[b] Resonances of the N-terminal amide group of the folded state could not be located. Resonances of the N-terminal two residues and the C-terminal three residues of the unfolded state could also not be located and no exchange peaks were observed to assigned resonances of the folded state for these residues.

isolated drkN SH3 in 50 mM sodium phosphate, 50 mM Na_2SO_4, pH 6, 25 °C. The use of Na_2SO_4 and the lower temperature were found to prevent precipitation of the sample due to aggregation of the unfolded state over time in the concentrated NMR sample. In addition to diagonal peaks at $^{15}N(\mathbf{f})_i$,$^{15}N(\mathbf{f})_i$,$^{1}HN(\mathbf{f})_i$, two cross peaks are observed for most residues in the folded state (**f**), including the exchange peak from the unfolded state (**u**) at $^{15}N(\mathbf{u})_i$,$^{15}N(\mathbf{f})_i$,$^{1}HN(\mathbf{f})_i$ and the sequential TOCSY-NOESY peak within the folded state at $^{15}N(\mathbf{f})_i$,$^{15}N(\mathbf{f})_{i+1}$,$^{1}HN(\mathbf{f})_{i+1}$. In addition, a third cross peak is sometimes seen, representing the exchange TOCSY-NOESY peak between the folded and unfolded states, at $^{15}N(\mathbf{u})_i$, $^{15}N(\mathbf{f})_{i+1}$, $^{1}HN(\mathbf{f})_{i+1}$. Cross peaks arising from cross-strand NOE transfers were also observed in a few cases. While the ^{15}N HSQC-TOCSY-NOESY- HSQC could also provide sequential cross peaks for resonances of the unfolded state, in practice only diagonal peaks at $^{15}N(\mathbf{u})_i$,$^{15}N(\mathbf{u})_i$,$^{1}HN(\mathbf{u})_i$ and exchange peaks at $^{15}N(\mathbf{f})_i$,$^{15}N(\mathbf{u})_i$,$^{1}HN(\mathbf{u})_i$ were observed for many residues. Sequential TOCSY-NOESY cross peaks for the unfolded form at $^{15}N(\mathbf{u})_i$,$^{15}N(\mathbf{u})_{i+1}$,$^{1}HN(\mathbf{u})_{i+1}$ were observed for only 40% of the residues for which they were seen in the folded state. Sequential exchange TOCSY-NOESY peaks, at $^{15}N(\mathbf{f})_i$,$^{15}N(\mathbf{u})_{i+1}$,$^{1}HN(\mathbf{u})_{i+1}$ or $^{15}N(\mathbf{u})_i$,$^{15}N(\mathbf{f})_{i+1}$,$^{1}HN(\mathbf{f})_{i+1}$ were even more rarely observed. The small number of sequential connectivities in the unfolded state is due to the lack of stable extended structure which would allow for efficient magnetization transfer via strong $C^{\alpha}H_i$,NH_{i+1} NOEs. Selected amide strips from the ^{15}N HSQC-TOCSY-NOESY-HSQC experiment are shown in Fig. 4. A summary of the sequential correlations derived from the NOESY-HSQC and ^{15}N HSQC-TOCSY-NOESY-HSQC experiments is shown in Fig. 5. The figure illustrates the use of the ^{15}N HSQC-TOCSY-NOESY-HSQC data in making two sequential connections (Thr^{22} to Glu^{23}, Lys^{56} to Asn^{57}) and resolving ambiguities in five other sequential assignments (His^{7} to Asp^{8}, Leu^{17} to Ser^{18}, Ser^{18} to

TABLE 2
BACKBONE CHEMICAL SHIFTS (ppm) OF THE FOLDED STATE OF THE drkN SH3 DOMAIN[a]

Residue	NH	^{15}N	H^{α}	Residue	NH	^{15}N	H^{α}
Met[1]	[b]	[b]	4.16	Glu[31]	8.08	122.0	4.38
Glu[2]	8.93	125.8	5.26	Asp[32]	8.41	121.9	4.47
Ala[3]	8.93	122.4	4.98	Asp[33]	8.22	119.3	4.69
Ile[4]	8.80	119.6	4.74	Ser[34]	8.11	116.2	4.53
Ala[5]	8.76	128.6	4.47	Asn[35]	8.88	120.1	4.59
Lys[6]	9.40	125.9	4.30	Trp[36]	7.98	121.8	5.20
His[7]	7.58	114.6	4.67	Tyr[37]	8.95	121.2	5.37
Asp[8]	8.72	121.2	4.71	Arg[38]	8.71	122.0	4.93
Phe[9]	8.58	122.0	4.69	Ala[39]	9.50	131.9	5.47
Ser[10]	7.60	124.2	4.41	Glu[40]	8.90	118.8	5.46
Ala[11]	8.24	128.0	3.87	Leu[41]	8.89	126.5	4.71
Thr[12]	8.71	113.4	4.39	Asp[42]	9.62	130.1	4.39
Ala[13]	7.41	124.2	4.59	Gly[43]	9.02	105.2	3.68/4.23
Asp[14]	8.58	119.7	4.41	Lys[44]	7.90	123.0	4.68
Asp[15]	8.18	115.3	4.73	Glu[45]	8.43	120.9	5.78
Glu[16]	7.39	119.4	5.15	Gly[46]	8.80	108.6	3.95/4.16
Leu[17]	8.43	125.0	4.72	Ile[47]	9.22	121.0	5.44
Ser[18]	7.84	117.9	4.76	Ile[48]	9.37	113.2	5.14
Phe[19]	8.62	115.3	4.97	Pro[49]	–	–	5.18
Arg[20]	9.37	119.9	5.09	Ser[50]	7.84	120.3	4.56
Lys[21]	9.23	121.0	4.22	Asn[51]	8.34	116.0	4.74
Thr[22]	8.75	117.8	4.52	Tyr[52]	7.63	119.4	4.65
Gln[23]	8.14	121.3	4.32	Ile[53]	7.22	111.6	5.24
Ile[24]	8.15	121.0	4.80	Glu[54]	8.74	121.1	4.80
Leu[25]	9.04	128.5	4.65	Met[55]	8.96	125.9	4.58
Lys[26]	8.22	122.6	4.68	Lys[56]	8.62	124.4	4.38
Ile[27]	8.40	125.2	4.20	Asn[57]	8.50	121.3	4.73
Leu[28]	9.19	129.3	4.43	His[58]	8.26	118.8	4.76
Asn[29]	7.61	114.6	4.80	Asp[59]	8.27	127.8	4.44
Met[30]	8.77	124.0	4.43				

[a] Assignments made in 50 mM sodium phosphate, 400 mM Na_2SO_4, pH 6, 25 °C, with water at 4.77 ppm as internal reference.

[b] Resonances of the N-terminal amide group and the C-terminal residue could not be located.

Phe[19], Ile[24] to Leu[25], Lys[26] to Ile[27].

Nearly complete assignments could be made using data from the HSQC-TOCSY-NOESY-HSQC experiment in conjunction with previously recorded NOESY-HSQC and TOCSY-HSQC experiments. A NOESY-HSQC experiment on a 1 mM sample of the drkN SH3 in 0.4 M Na_2SO_4, 50 mM sodium phosphate, pH 6, 25 °C was recorded in order to confirm the assignments. The addition of Na_2SO_4, at the extreme end of the Hofmeister series of inorganic anions known to stabilize protein structure (Arakawa and Timasheff, 1985) led to a completely folded conformation having no observable exchange with the unfolded state. Although the chemical shift changes relative to spectra recorded on samples without Na_2SO_4 were very small, HSQC spectra with incremental additions of 50 mM Na_2SO_4 were recorded to enable unambiguous correlation of

assignments at the different Na_2SO_4 concentrations. The backbone ^1H and ^{15}N assignments for folded and unfolded states of drkN SH3 in 50 mM sodium phosphate, pH 6 and 30 °C are given in Table 1, and the backbone assignments for the folded drkN SH3 in the presence of 0.4 M Na_2SO_4 are presented in Table 2. There are no significant differences between the chemical shifts of the two folded states, reflecting the absence of averaging of chemical shifts from exchanging forms of the SH3 in samples without Na_2SO_4.

CONCLUSIONS

We have assigned the backbone ^1H and ^{15}N resonances of both folded and unfolded states of the 59-residue drkN SH3 domain using heteronuclear ^{15}N-edited pulsed field gradient experiments which exploit the ^{15}N chemical shift dispersion of unfolded proteins and minimize saturation and dephasing of water. By minimizing the perturbation of water, decreases in the intensity of resonances of the rapidly exchanging amide protons of the unfolded state have been prevented. These experiments should prove extremely useful for studies of conformationally fluctuating states of proteins or protein fragments. The HSQC-TOCSY-NOESY-HSQC experiment may be helpful for assignment in cases where the ^{15}N chemical shift dispersion is greater than that of ^1H resonances. In addition, the described experiments could be favorably applied to any protein system, especially if studies must be performed at pH values near or above neutral, where amide exchange may also lead to significant loss of intensity of amides and other resonances.

ACKNOWLEDGEMENTS

The authors thank Randall Willis for technical assistance in protein expression and purification, Dr. Ranjith Muhandiram for assistance in performing some of the NMR experiments described and Dr. Tony Pawson for his enthusiastic support of the project and for making available expertise in his laboratory for the subcloning of the drkN SH3 domain. O.Z. acknowledges an Open Fellowship from the University of Toronto and J.P.O. acknowledges support from the National Cancer Institute of Canada (NCIC). This work was funded through a grant from the NCIC (J.D.F. and L.E.K.) with funds from the Canadian Cancer Society.

NOTE ADDED IN PROOF

In the pulse schemes of Fig. 1 we now prefer to exorcycle the ^{15}N 180° pulse applied during the period in which the ^{15}N chemical shift is recorded. In this case the phase of the ^{15}N 90° pulse immediately preceding this 180° pulse is not phase cycled +,−. Note that the phase of the receiver is inverted when the phase of the ^{15}N 180° pulse is incremented by 90°.

It has recently come to our attention that Stonehouse et al. (*J. Magn. Reson. Ser. A*, **107**, 178–184, 1994) have also noted the importance of minimizing water saturation and dephasing through the use of water-selective pulses.

REFERENCES

Alexandrescu, A.T., Abeygunawardana, C. and Shortle, D. (1994) *Biochemistry*, **33**, 1063–1072.
Arakawa, T. and Timasheff, S.N. (1985) *Methods Enzymol.*, **114**, 49–77.
Bax, A. and Pochapsky, S. (1992) *J. Magn. Reson.*, **99**, 638–643.

Booker, G.W., Breeze, A.L., Downing, A.K., Panayotou, G., Gout, I., Waterfield, M.D. and Campbell, I.D. (1992) *Nature*, **358**, 684–687.
Cavanagh, J. and Rance, M. (1992) *J. Magn. Reson.*, **96**, 670–678.
Cicchetti, P., Mayer, B.J., Thiel, G. and Baltimore, D. (1992) *Science*, **257**, 803–806.
Delaglio, F., NMRPipe Software System, National Institutes of Health, Bethesda, MD, 1993.
Evans, P.A., Topping, D.D., Woolfson, D.N. and Dobson, C.M. (1991) *Proteins*, **9**, 248–266.
Garrett, D.S., Powers, R., Gronenborn, A.M. and Clore, G.M. (1991) *J. Magn. Reson.*, **95**, 214–220.
Grzesiek, S. and Bax, A. (1993) *J. Am. Chem. Soc.*, **115**, 12593–12594.
Kay, L.E., Keifer, P. and Saarinern, T. (1992) *J. Am. Chem. Soc.*, **114**, 10663–10665.
Kay, L.E., Xu, G.Y. and Yamazaki, T. (1994) *J. Magn. Reson. Ser. A*, **109**, 129–133.
Khoda, D., Hatanaka, H., Odaka, M., Mandiyan, V., Ullrich, A., Schlessinger, J. and Inagaki, F. (1993) *Cell*, **72**, 953–960.
Koch, C.A., Anderson, D., Moran, M.F., Ellis, C. and Pawson, T. (1991) *Science*, **252**, 668–674.
Koyama, S., Yu, H., Dalgarno, D.C., Shin, T.B., Zydowdky, L.D. and Schreiber, S.L. (1993) *Cell*, **72**, 945–952.
Logan, T.M., Olejnickzak, E.T., Xu, R.X. and Fesik, S.W. (1993) *J. Biomol. NMR*, **3**, 225–231.
Logan, T.M., Thériault, Y. and Fesik, S.W. (1994) *J. Mol. Biol.*, **236**, 637–648.
Lumb, K.J. and Kim, P.S. (1994) *J. Mol. Biol.*, **236**, 412–420.
Marion, D., Ikura, M., Tschudin, R. and Bax, A. (1989) *J. Magn. Reson.*, **85**, 393–399.
McCoy, M.A. and Mueller, L. (1992) *J. Am. Chem. Soc.*, **114**, 2108–2110.
Mueller, L., Campbell-Burke, S. and Domaille, P. (1992) *J. Magn. Reson.*, **96**, 408–415.
Muhandiram, D.R. and Kay, L.E. (1994) *J. Magn. Reson. Ser. B*, **103**, 203–216.
Musacchio, A., Gibson, T., Lehto, V.-P. and Saraste, M. (1992a) *FEBS Lett.*, **307**, 55–61.
Musacchio, A., Noble, M., Paupit, R., Wierenga, R. and Saraste, M. (1992b) *Nature*, **359**, 851–855.
Neri, D., Billeter, M., Wider, G. and Wüthrich, K. (1992) *Science*, **257**, 1559–1563.
Noble, M.E.M., Musacchio, A., Saraste, M., Courtneidge, S.A. and Wierenga, R.K. (1993) *EMBO J.*, **12**, 2617–2624.
Olivier, J.P., Raabe, T., Henkemeyer, M., Dickson, B., Mbamalu, G., Margolis, B., Schlessinger, J., Hafen, E. and Pawson, T. (1993) *Cell*, **73**, 179–191.
Palmer, A.G., Cavanagh, J., Wright, P.E. and Rance, M. (1991) *J. Magn. Reson.*, **93**, 151–170.
Pawson, T. and Gish, G.D. (1992) *Cell*, **71**, 359–362.
Schleucher, J., Sattler, M. and Griesinger, C. (1993) *Angew. Chem.*, **114**, 1518–1521.
Shaka, A.J., Keeler, J., Frenkiel, T. and Freeman, R. (1983) *J. Magn. Reson.*, **52**, 335–338.
Simon, M.A., Dodson, G.S. and Rubin, G.M. (1993) *Cell*, **73**, 169–177.
States, D.J., Haberkorn, R. and Ruben, D.J. (1982) *J. Magn. Reson.*, **48**, 286–292.
Yang, Y.S., Garbay, C., Duchesne, M., Cornille, F., Jullian, N., Fromage, N., Tocque, B. and Roques, B.P. (1994) *EMBO J.*, **13**, 1270–1279.
Yu, H., Rosen, M.K., Shin, T.B., Seidel-Duggan, C., Brugge, J.S. and Schreiber, S.L. (1992) *Science*, **258**, 1665–1668.
Yu, H., Chen, J.K., Feng, S., Dalgarno, D.C., Brauer, A.W. and Schreiber, S.L. (1994) *Cell*, **76**, 933–945.
Zhang, O. and Forman-Kay, J.D. (1994) *Biochemistry*, submitted for publication.